JOURNAL OF GEOPHYSICAL RESEARCH, VOL. 104, NO. C1, PAGES 1361–1375, JANUARY 15, 1999

Upper layer currents in the western tropical North Atlantic (1989–1991)

B. Bourles
Centre ORSTOM de Brest, Plouzane, France

R. L. Molinari, E. Johns, and W. D. Wilson
Atlantic Oceanographic and Meteorological Laboratory, Physical Oceanography Division, NOAA, Miami, Florida

K. D. Leaman
Rosenstiel School of Marine and Atmospheric Sciences, University of Miami, Miami, Florida

Abstract. Shipboard acoustic Doppler current profiler (ADCP) measurements and hydrographic observations of temperature, salinity, and dissolved oxygen are used to examine the upper water column flow field in the North Brazil Current (NBC) retroflection region of the western tropical Atlantic Ocean. Observations are presented from six cruises, one conducted in August 1989 and the other five conducted during the Western Tropical Atlantic Experiment between January 1990 and September 1991. The upper water column is divided into two layers, an upper thermocline layer located between the surface and the 24.5 σ_θ isopycnal surface and a lower subthermocline layer located between the 24.5 and 26.75 isopycnals. In the upper layer the NBC retroflects north of the equator to form the eastward flowing North Equatorial Countercurrent (NECC). During the six cruises the retroflection appeared complete. However, data coverage did not extend shoreward of the 200-m isobath, so the possibility of a continuous flow over the shelf still remains. There were also indications of several NBC rings that had apparently separated from the NBC retroflection and drifted to the northwest toward the eastern Caribbean Sea. North of the NBC retroflection and the NECC, the North Equatorial Current (NEC) flows west as the southern limb of the subtropical gyre. Part of the NEC is observed to retroflect cyclonically to join the eastward NECC flow. In the lower layer, beneath the NBC, the North Brazil Undercurrent retroflects to feed the eastward North Equatorial Undercurrent (NEUC). To the north a deeper component of the NEC recurves to also contribute to the NEUC.

1. Introduction

Circulation patterns within the western tropical Atlantic Ocean play an important role in the interhemispheric transport of mass, heat, and salt [*Schmitz and Richardson*, 1991; *Schmitz et al.*, 1993; *Schmitz and McCartney*, 1993]. The Deep Western Boundary Current (DWBC) transports cold North Atlantic Deep Water toward the southern hemisphere. The North Brazil Current (NBC) transports warm surface waters northward to close the thermohaline overturning cell [e.g., *Gordon*, 1986]. The magnitude of this cross-equatorial exchange has been estimated by *Schmitz and Richardson* [1991] to be of the order of 13 Sv (1 Sv = 10^6 m^3 s^{-1}).

In addition to the DWBC and the NBC, the mean circulation in this region is complicated by the presence of zonal countercurrents and other western boundary currents. These currents may also have a role in regional and global climate. For example, in the Pacific, *Gu and Philander* [1997] propose shallow overturning cells in both hemispheres that connect the tropical and subtropical basins and are coupled to the overlying atmosphere. The oceanic component of this coupled mode is characterized by subduction of near-surface waters in the subtropics. In the northern hemisphere the subducted water is advected westward by the southern limb of the subtropical gyre, the North Equatorial Current (NEC). In the *Gu and Philander* [1997] model, at the western boundary, the NEC bifurcates, a portion of its transport continuing to flow westward into the subtropical gyre and another portion turning back to the east after becoming entrained in the Equatorial Undercurrent (EUC). The EUC waters upwell and are transported poleward to the subtropical gyre by Ekman processes, thus closing the cell. In contrast to this Pacific model, we portray the retroflected portion of the Atlantic NEC becoming entrained into the North Equatorial Countercurrent (NECC) and the North Equatorial Undercurrent (NEUC) in Figure 1.

As shown in pioneering studies by *Metcalf and Stalcup* [1967], *Metcalf* [1968], and *Cochrane et al.* [1979], the vertical structure of the circulation is also rather complex. The NBC and its subsurface component, the North Brazil Undercurrent (NBUC [*Silveira et al.*, 1994]), advect southern hemispheric waters across the equator and feed subsurface eastward currents at different latitudes and different depths. These zonal currents include the North Equatorial Countercurrent, located in the near-surface layer, the Equatorial Undercurrent, centered at the thermocline, and the North Equatorial Undercurrent, located below the thermocline (Figure 1). As described

Paper number 1998JC900025.
0148-0227/99/1998JC900025$09.00

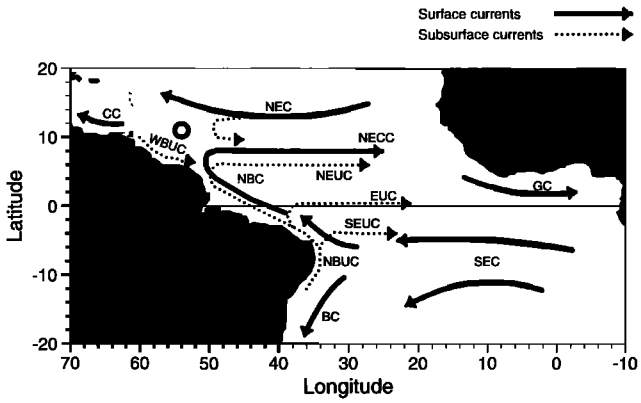

Figure 1. Schematic diagram of the mean surface and subsurface currents in the tropical Atlantic Ocean (adapted from *Richardson et al.* [1994]). Abbreviations are NEC, North Equatorial Current; CC, Caribbean Current; WBUC, Western Boundary Undercurrent; NECC, North Equatorial Countercurrent; NBC, North Brazil Current; NEUC, North Equatorial Undercurrent; EUC, Equatorial Undercurrent; GC, Guinea Current; SEUC, South Equatorial Undercurrent; NBUC, North Brazil Undercurrent; SEC, South Equatorial Current; and BC, Brazil Current.

previously, these eastward flows may also be fed by a branch of the NEC. A southeastward undercurrent, the Western Boundary Undercurrent (WBUC [*Flagg et al.*, 1986; *Johns et al.*, 1990; *Colin and Bourles*, 1994]), has been observed to flow along the boundary from the eastern Caribbean to also join the NEUC (Figure 1).

Superimposed on these mean features, large spatial and temporal variability over the entire water column adds to the complexity of the area. For example, temporal variability on a seasonal timescale is also significant in this region. During the summer/fall season when the Intertropical Convergence Zone (ITCZ) is at its northern extreme and the NECC is at maximum strength [*Garzoli*, 1992], *Richardson and Reverdin* [1987] and *Philander and Pacanowski* [1986] found that the entire NBC separated from the coast and retroflected eastward. Recent direct velocity measurements made during the summer season by *Wilson et al.* [1994] and subsurface float trajectories shown by *Richardson et al.* [1994] also suggest complete retroflection, although neither study adequately resolves the flow closet to the coast. However, in contrast to these observations, both *Csanady* [1985] in an empirical modeling study and *Schott and Boning* [1991] in a numerical modeling study found that during the summer/fall season, only a portion of the NBC transport retroflected, with the remainder continuing northwestward along the coast.

In the winter/spring season, when the ITCZ is at its southern extreme and the NECC is at minimum strength [*Garzoli*, 1992], both model estimates [*Philander and Pacanowski*, 1986] and surface drifter studies [*Richardson and Reverdin*, 1987] agree in suggesting that the NBC may flow continuously northwestward along the South American coastline to the Caribbean Sea. From a cruise carried out in March 1994, *Schott et al.* [1995] suggested that much of the NBC was flowing continuously along the boundary at that time. Similar northwestward flows beyond the retroflection region have been reported by *Johns et al.* [1990], *Schott and Boning* [1991], and *Schott et al.* [1993].

Determining the continuity of coastal flows in this region in the absence of extensive synoptic surveys is made difficult by the presence of rings that have separated from the NBC as it retroflects from the coast [*Cochrane et al.*, 1979; *Bruce et al.*, 1985; *Johns et al.*, 1990; *Richardson et al.*, 1994; *Fratantoni et al.*, 1995]. These NBC rings may have contributed to the observations of northwestward coastal currents and the presence of southern hemisphere origin waters well north of the retroflection region [*Richardson and Walsh*, 1986; *Richardson and Reverdin*, 1987]. The structure and behavior of the NBC retroflection and its associated boundary currents and rings, in particular, have been the subject of several recent investigations [*Johns et al.*, 1990; *Schott and Boning*, 1991; *Didden and Schott*, 1993; *Schott et al.*, 1993, 1995; *Richardson et al.*, 1994; *Colin and Bourles*, 1994; *Colin et al.*, 1994; *Fratantoni et al.*, 1995; *Schott et al.*, 1995].

Wilson et al. [1994] (hereinafter referred to as W94) used a combination of direct current observations from a hull-mounted acoustic Doppler current profiler (ADCP) and hydrographic data to study the upper layer circulation patterns and water mass characteristics in the region during a synoptic survey in August–September 1989. Many of the complexities in the regional current and water property fields described above were present during this survey and quantified by the W94 analysis. Using techniques similar to those employed by W94, we herein present additional synoptic descriptions of the upper layer circulation and water mass properties, using direct current velocity and hydrographic data from five other surveys carried out during the Western Tropical Atlantic Experiment (WESTRAX [*Brown et al.*, 1992]) in 1990 and 1991. For completeness, we also include the August 1989 cruise of W94 in the present study. We first present the available data, then describe our transport calculations and water mass determinations. We consider the main current structures, along with the water mass properties, through horizontal current fields and vertical sections. Transports are calculated within two isopycnal layers located above and below the thermocline. Schematic transport diagrams for each cruise and each layer are constructed and used to summarize the transport and water mass results.

2. Data

The data used in this study were collected in 1989, 1990, and 1991 in the region bounded by the equator and 15°N, between 40°W and 70°W. Track lines and hydrographic station locations for the six cruises considered herein are shown in Figure 2. Dates of each cruise and types of data collected are summarized in Table 1. The timing of the cruises was dictated primarily by vessel availability rather than by scientific considerations.

2.1. Conductivity-Temperature-Depth-Oxygen Data

Pressure, temperature, salinity (expressed as Practical Salinity Scale 1978), and dissolved oxygen measurements were collected with a Neil Brown Instruments Mark III $CTDO_2$ system at station locations indicated in Figure 2. The conductivity-temperature-depth (CTD) pressure, temperature, conductivity, and oxygen sensors were calibrated in the laboratory before and after each cruise. Water samples collected concurrently with the $CTDO_2$ data were used to provide additional calibration for the conductivity and oxygen sensors. A description of the $CTDO_2$ unit, data reduction techniques, accuracies, and water sample analyses have been described by *Wilburn et al.* [1990] and *Johns and Wilburn* [1993a, b]. Temperature, salinity,

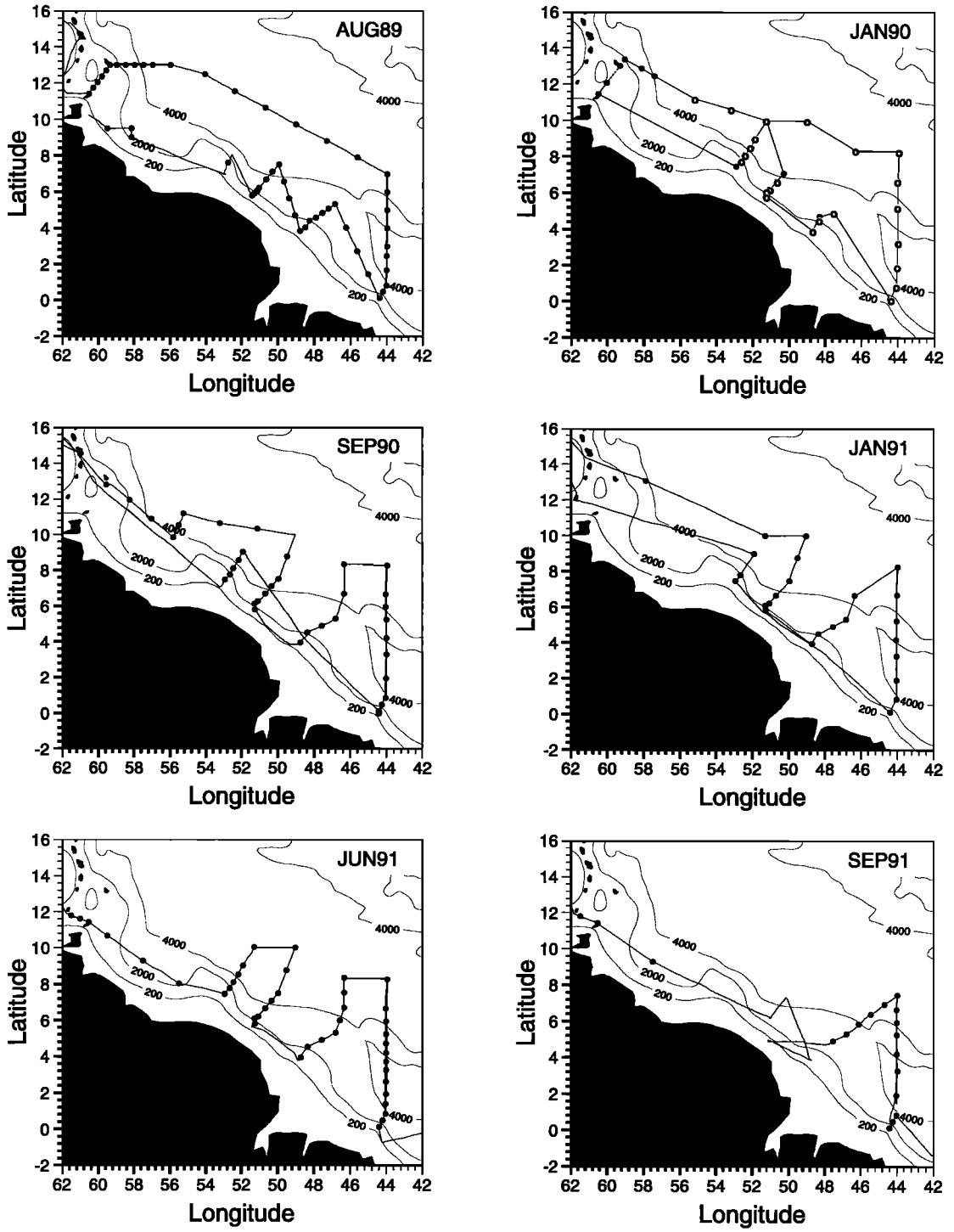

Figure 2. Cruise maps of the six cruises considered in this study: August 1989, January 1990, September 1990, January 1991, and September 1991. Shipboard acoustic Doppler current profiler (ADCP) measurements were taken along all cruise track lines except January 1990. Solid circles represent conductivity-temperature-depth-O_2 ($CTDO_2$) profiles, and open circles represent $CTDO_2$ and Pegasus profiles taken during January 1990.

pressure, and oxygen accuracies are of the order of ±0.005°C, ±0.004, ±3 dbar and ±0.06 mL L^{-1}, respectively.

2.2. Shipboard ADCP Data

Shipboard ADCP observations were collected continuously along the track lines during all cruises except January 1990 (Table 1 and Figure 2). The ADCP provided nearly continuous coverage of the upper ocean velocity field. Velocity data relative to the ship were collected as averages over 8-m vertical bins, with the center of the first bin at 14 m. The original 1-min mean values have been edited and further averaged into 15-min values for this analysis. Absolute referencing was provided

Table 1. WESTRAX Cruise Data Collection

Cruise Dates	$CTDO_2$	ADCP	Pegasus[a]
Aug. 28 to Sept. 15, 1989	54	yes	4
Jan. 31 to Feb. 19, 1990	33	no	24
Sept. 17 to Oct. 4, 1990	47	yes	27
Jan. 16–28, 1991	25	yes	24
June 20 to July 3, 1991	43	yes	26
Sept. 7–18, 1991	18	yes	7

[a]Only Pegasus data collected during the January 1990 cruise are used in this study.

by the Global Positioning System (GPS), augmented with the TRANSIT satellite when the former was unavailable. The shipboard system was calibrated during each cruise as described by *Joyce* [1989] and *Pollard and Read* [1989], and the accuracy of the mean profiles is better than 5 cm s^{-1}. Gyrocompass-induced transient errors as large as 3 to 7 cm s^{-1}, as described by W94, may remain in the data set but will tend to average out over the long transport sections described here. Further details of the data acquisition and processing methodology are given by *Wilson and Routt* [1992] and *Routt and Wilson* [1992].

2.3. Pegasus Velocity Profiler Data

Absolute horizontal current components were also obtained during the five WESTRAX cruises with a free-falling Pegasus profiler [*Spain et al.*, 1981; *Leaman and Vertes*, 1983]. However, only Pegasus data from the January 1990 effort were used for this analysis (see Figure 2 for station locations), as ADCP data were not available for that particular cruise. Systematic measurement errors are due to uncertainties in the different parameters used to determine the position of the Pegasus, which is acoustically tracked by two transponders placed on the ocean floor [*Leaman and Vertes*, 1983]. Errors are also due to internal waves, which cause differences between the descending and ascending profiles [*Send*, 1994]. These uncertainties are of the same order as the systematic measurement errors. Total errors rarely exceed 10% of the velocity magnitude in the upper layers, decreasing to 5% with depth [*Leaman et al.*, 1987; *Send*, 1994; *Colin and Bourles*, 1994; *Leaman et al.*, 1995].

2.4. Comparison of ADCP and Pegasus Currents

A comparison between ADCP and Pegasus currents and transport estimates provides both a demonstration of the similarity of these measurements and another measure of their uncertainty. Figure 3 shows the zonal component of the velocity across the 44°W section, from the equator to around 8°N, as observed from ADCP and Pegasus measurements in June 1991. Selected isopycnal surfaces as computed from the hydrographic stations are superimposed on the velocity sections. Visually, the structures of the principal current cores are remarkably similar for both instruments, and the velocity extrema are comparable. However, owing to varying station resolution (the ADCP provides nearly continuous coverage of the velocity field, while the Pegasus data are obtained only at the station locations indicated by the double arrows in Figure 3, bottom) the comparison is not as exact for other features. For example, the large area of positive velocity in Figure 3 (top) between 800 and 1000 km is not present in Figure 3 (bottom) below about 100 m depth. Also, the peak speed of the NECC is found to be 120 cm s^{-1} in a subsurface core as measured by the ADCP and only 100 cm s^{-1} as measured by Pegasus. Nevertheless, for the most part, the velocity comparison shows that the two methods are generally in agreement. Transport intercomparisons for the 44°W section for the five cruises with both ADCP and Pegasus data collection yielded a mean transport difference of only 1.5 Sv, supporting the relative interchangeability of the two measurement types for computing transport.

2.5. Transport Calculations

The ADCP data and Pegasus measurements are used to estimate the transports within two density layers defined in section 3. As the ADCP data provided better time and space resolution over the upper several hundred meters of the water column, we used Pegasus measurements only for the January 1990 cruise when no ADCP data were collected. ADCP sections were computed by averaging the 15-min profiles onto a 10-km horizontal by 10-m vertical grid along the cruise track. For transport calculations we extended the first bin velocity to the surface; where the deepest velocity measurements were shallower than the deeper isopycnal layer depth (a rare occur-

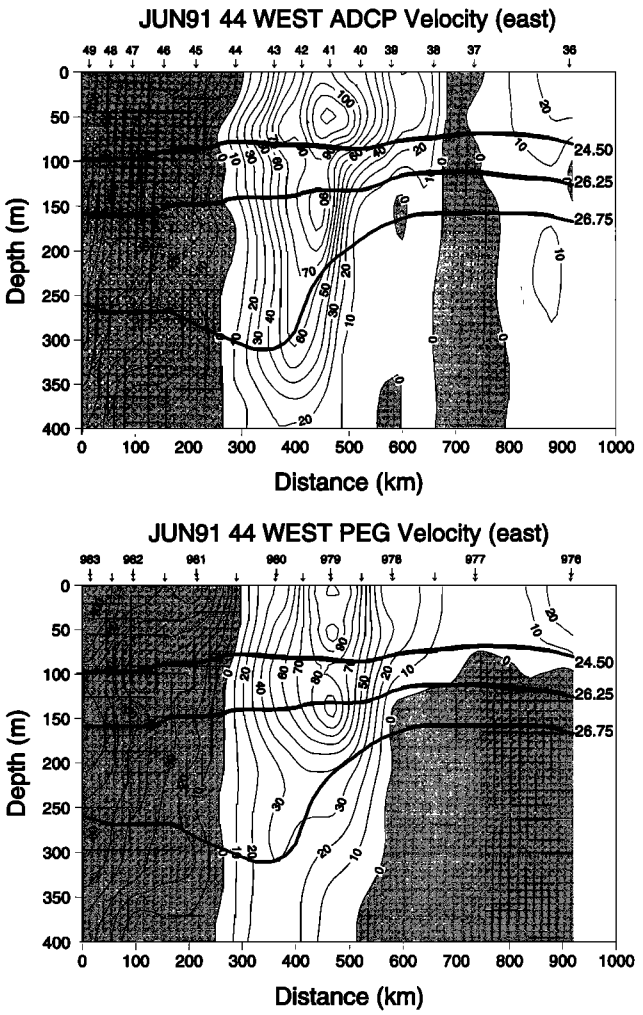

Figure 3. Vertical sections of eastward velocity in centimeters per second obtained in June 1991 along 44°W from (top) ADCP, with numbers at top denoting CTD data, and (bottom) Pegasus, with station numbers indicated at top. Shaded flow is to the west. Distance is in kilometers from the transect origin at 0°, 44°W.

rence), we extrapolated the deep velocity to fill the layer. Pegasus transports were calculated in a similar way, with the first measurement usually located between the surface and 20 m. No deep extrapolation was necessary in this case, as Pegasus profiles generally extend to the bottom.

The upper ocean water column was divided into two layers based on the CTD-derived density structure, following W94. The upper layer is bounded by the sea surface and the 24.5 isopycnal surface, approximately corresponding to the 24°C isotherm, and typically includes the velocity cores of the NBC and the NECC (Figure 3). The lower layer, below the thermocline, is bounded by the 24.5 and 26.75 isopycnal surfaces (approximately corresponding to the 24° to 12°C isotherms) and includes the velocity cores of the NBUC and the NEUC. Transports were calculated for each density layer and each transect by spatial integration of the velocity component perpendicular to the transects.

3. Regional Water Masses

Source regions for the water masses in the deeper layer (σ_θ = 24.5 to 26.75) can be clearly distinguished by their temperature, salinity, and oxygen properties. *Metcalf and Stalcup* [1967] and *Metcalf* [1968] pointed out differences between the relative salinity maxima of the NBC and northern hemisphere origin coastal currents (Figure 1) to suggest a lack of connectivity between the flows. Similarly, they used the difference in oxygen concentrations between the northern (low oxygen) and southern (high oxygen) hemisphere Atlantic waters to show the feeding of the EUC by southern hemispheric waters that had been transported into the region by the NBC.

More recently, W94 used salinity and oxygen patterns observed in August–September 1989 to distinguish three water masses encountered in the upper layers of the western tropical North Atlantic. The first water mass is the Subtropical Underwater (SUW), formed in the northern hemisphere and characterized by high salinity values with relatively high oxygen concentrations above the thermocline. The source of the SUW is the high evaporation region of the subtropics to the north of the study area. These waters are then advected southward and westward within the subtropical anticyclonic gyre [*Worthington*, 1976].

The second water mass described by W94, the South Atlantic counterpart of the SUW, also exhibits high salinity values above the thermocline in its source region but has lower salinity values than the northern SUW by the time it has reached the study region. Regionally, southern SUW has the highest oxygen concentrations over the entire upper ocean water column.

A third water mass commonly found in the study area has its source in the eastern tropical Atlantic [*Emery and Dewar*, 1982]. This water mass is carried into the western tropical Atlantic by the southern edge of the NEC and the northern edge of the South Equatorial Current (SEC). Eastern tropical Atlantic water (ETW) has markedly lower salinity above the thermocline than the northern SUW, similar in magnitude to the southern SUW in the study area, but is easily distinguished by its very low oxygen concentration.

Following the methods used by W94, the three regional source water masses were defined by their salinity-oxygen correlation on the density surface where σ_θ equals 26.25. This isopycnal is located at the bottom of the main thermocline, at a potential temperature of 16° to 18°C. At this level, combining

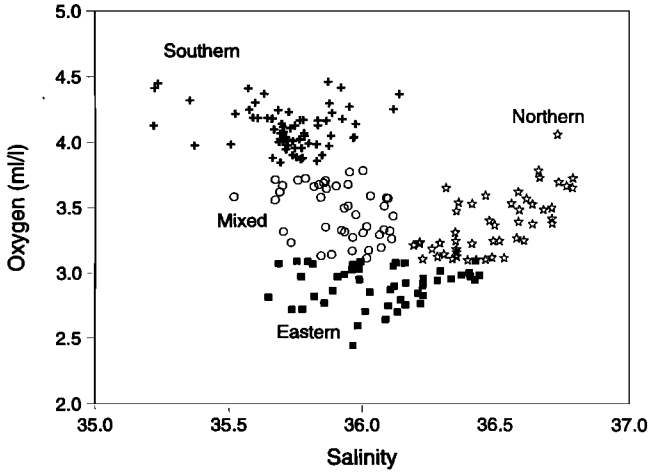

Figure 4. Salinity-dissolved oxygen correlation on the σ_θ = 26.25 isopycnal surface for the combined six Western Tropical Atlantic Experiment (WESTRAX) cruises. Symbols refer to water mass origin. Crosses represent the high-oxygen waters of the southern hemisphere (labeled southern); solid squares are the low-oxygen eastern tropical water (labeled eastern); open circles are a mixture of the southern and eastern tropical water types (labeled mixed); and stars are the northern Subtropical Underwater (labeled northern).

all stations from the six cruises, the three primary water masses are clearly distinguishable (Figure 4). North Atlantic SUW has the highest salinity and intermediate oxygen; South Atlantic SUW has low salinity and the highest oxygen; and eastern tropical water has the lowest oxygen. A mixture of these water masses occurs mostly along the edge of the NBC between the southern and eastern origin water masses (W94). The open area on the salinity-oxygen correlation plot in the high-oxygen/moderate-to-high-salinity range, i.e., the "v"-shaped distribution of points in Figure 4, implies that a direct mix between "pure" southern and "pure" northern SUW waters rarely occurs in the region.

Having defined the three water masses by their salinity-oxygen correlation on the 26.25 density surface, it is possible to go back to the full water column properties and compute average temperature-salinity and temperature-oxygen curves for each designated water mass (Figure 5). The water mass differentiation can be seen to apply over a large portion of the upper water column, at all densities greater than about 25.0 (temperatures <24°C), down to at least a density of 27.0 (about 12°C). Thus the water mass designations extend over a larger portion of the water column than only at the 26.25 isopycnal surface and can be used to differentiate water masses in the entire σ_θ = 24.5 to 26.75 portion of the water column.

We will consider a fourth water mass in our discussions of the lower layer. As described above, Figure 4 includes S-O_2 points that represent a mixture of ETW and southern hemisphere water. This mixture of water masses will serve as the fourth component of the regional hydrography.

In the surface layer of the region (i.e., surface to σ_θ = 24.5), water mass sources are difficult to discern from only $CTDO_2$ measured parameters. In particular, the average θ-S and θ-O_2 curves all coalesce above about 25°C (Figure 5). Close to the air-sea interface, the influence of local river discharges (e.g., the Amazon), evaporation and precipitation, and surface temperature effects on oxygen saturation concentrations all con-

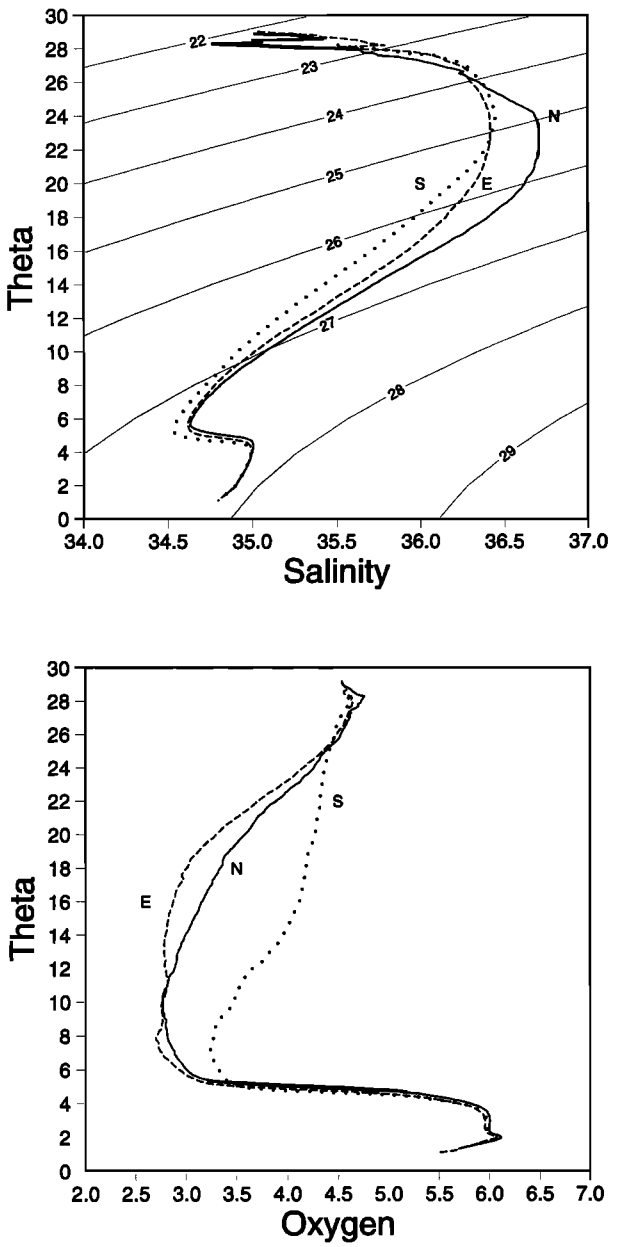

Figure 5. Average potential temperature versus (top) salinity and (bottom) dissolved oxygen for the water masses as defined in Figure 4 for the combined six cruises. Abbreviations are N, northern hemisphere Subtropical Underwater (SUW); E, eastern tropical Atlantic water; and S, southern hemisphere SUW.

tribute to the complicated near-surface water mass distribution. As a first approximation therefore, properties close to the σ_θ = 24.5 surface are assumed to be representative of the entire upper water column. We recognize the weaknesses in this approach, such as including transport of 20-m-thick Amazon water lenses in a pure water mass transport estimate, but wish to retain a manageable number of water mass types.

4. Results

4.1. Horizontal Fields of Currents

The major currents of the region can be examined by means of plan-view maps of velocity vectors averaged over the two density layers. The horizontal current fields as measured using the shipboard ADCP for five cruises and the Pegasus velocity profiler for the January 1990 cruise are shown for the two density layers in Figures 6 and 7, with the water mass symbols as defined on the σ_θ = 26.25 isopycnal surface in Figure 4 given at each $CTDO_2$ station.

As in previous studies, the current fields portray a spatially complex mix of intense boundary currents, retroflections, zonal currents, and rings. Currents are most intense in the surface layer (Figures 6 and 7). As will be differentiated in the next section, the NBC in the upper and the NBUC in the lower layer advect southern hemisphere water into the study area. In both layers the northwestward extension of the southern hemisphere waters varies and is bounded by an anticyclonic turning of the boundary current (i.e., the retroflection of the NBC).

During all cruises the retroflection feeds eastward flows across 44°W (Figures 6 and 7). In the upper layer the NBC feeds the NECC. During the three summer and one spring cruise the NECC is composed of southern, mixed, and eastern origin water masses and is located between 2°N and 6°N. During the two winter cruises the NECC is composed of mixed and eastern origin water masses and is observed north of 6°N. In the lower layer the NBUC feeds the NEUC. The NEUC is located between 2°N and 6°N and, similarly to the NECC, is also fed by waters from both hemispheres.

To the north of the NBC/NECC retroflection system the NEC is present as a relatively broad westward flow in both layers with weaker maximum speeds than observed farther to the south in the NBC/NECC system (Figures 6 and 7). The northern flank of the NEC advects SUW and the southern flank ETW. The water mass distributions indicate that at least a portion of the NEC transport (ETW during these cruises) retroflects back to the east to become entrained in the NECC and NEUC during all six cruises.

As described in W94 for the August 1989 cruise, the WBUC is a subthermocline flow that also brings northern origin water masses into the region to join the eastward equatorial counterflows. During this cruise the WBUC exits the Caribbean (i.e., the eastward and southward flow at about 10°N, 60°W in the August 1989 panel of Figure 7) and eventually, after a rather tortuous path, ultimately becomes entrained in the NEUC. The situation is similar during the September 1990 cruise. The WBUC is not found on the other current charts.

NBC retroflection rings are best identified using water mass observations. Unfortunately, water mass data from the six cruises are somewhat limited north of the retroflection. Combining the limited hydrographic data with the ADCP data indicates that rings recently separated from the retroflection (i.e., stations with southern hemisphere waters that are separated from their source in the NBC retroflection by either mixed or northern origin properties) are present during the January 1990 and January 1991 cruises.

4.2. Vertical Sections of Currents

The structure and transport of the NBC, NBUC, NECC, and NEUC currents can be examined further by means of vertical sections of velocity. Vertical sections of the eastward velocity component through the common meridional section at 44°W are shown in Figure 8. Distances are given from the southernmost end of the section near 0°, 44°W. The isopycnals used to delineate the upper and lower layers are superimposed on the velocity contours, and the water mass types as defined on the

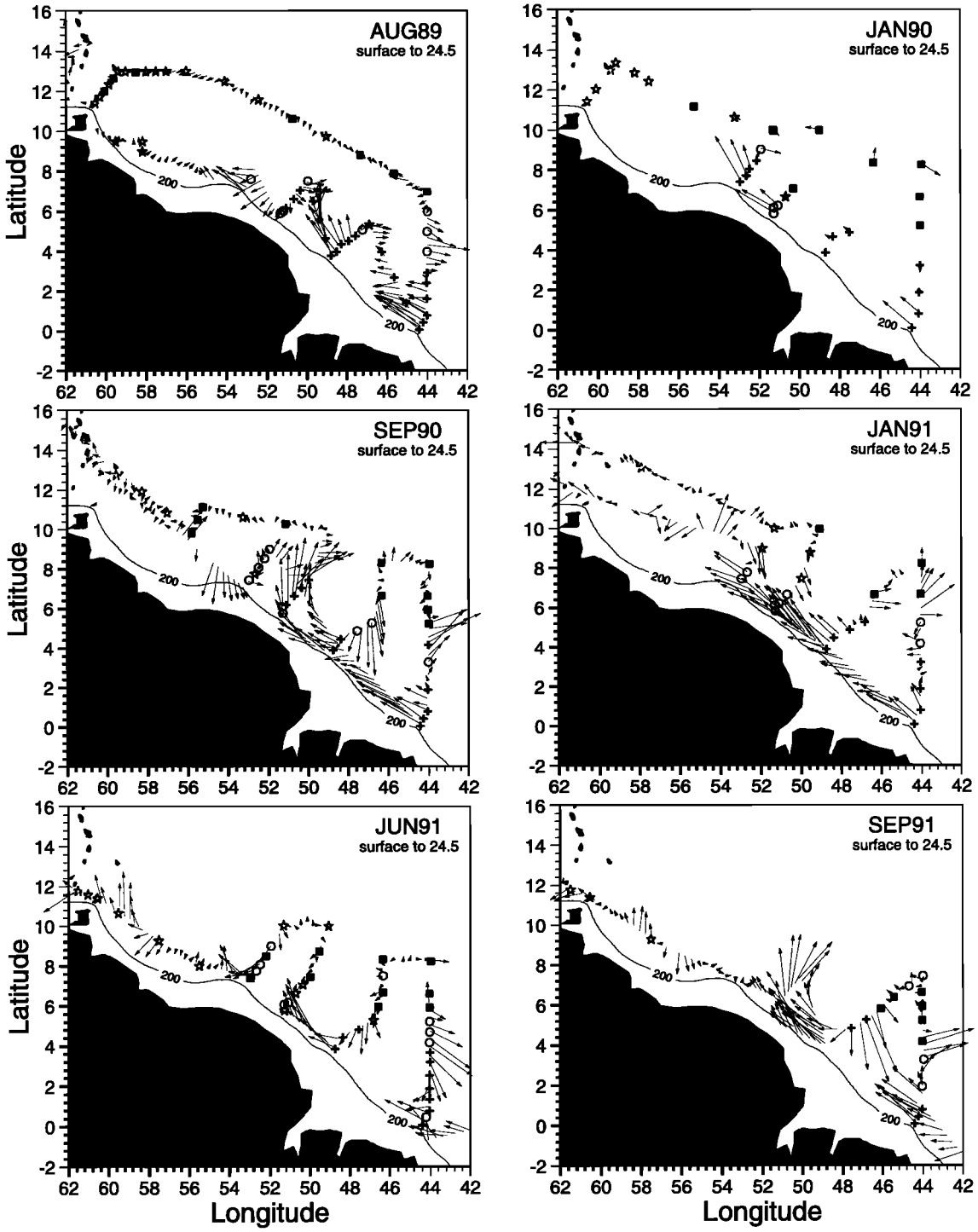

Figure 6. Vector maps of vertically integrated ADCP velocity (Pegasus velocity in January 1990), between the surface and the 24.5 isopycnal surface, for each cruise. The velocity vector scale is 1° longitude equals a speed of 50 cm s^{-1}. Symbols refer to water mass designations as defined in Figure 4.

26.25 isopycnal surface (also shown) are indicated at the $CTDO_2$ station locations.

The NBC appears as a surface-intensified flow with maximum speeds located above the 24.5 isopycnal surface on the southern edge of all the sections. With the exception of the two January sections, the NBC extends some 200 to 300 km offshore. During January 1990 and 1991, westward flow occupies nearly the entire southernmost 600 to 700 km of the 44°W transect. Maximum speeds of the NBC are typically found in the southernmost 50 km of the section. Peak speeds are observed during the spring and summer cruises, as high as 110 cm s^{-1} during September 1991, with lower maximum speeds (60–80 cm s^{-1}) observed during the two winter cruises.

Also on the southern edge of all the transects, intense westward flows (speeds greater than 30 cm s^{-1}) extend deeper into the water column (Figure 8). These deeper velocity maxima

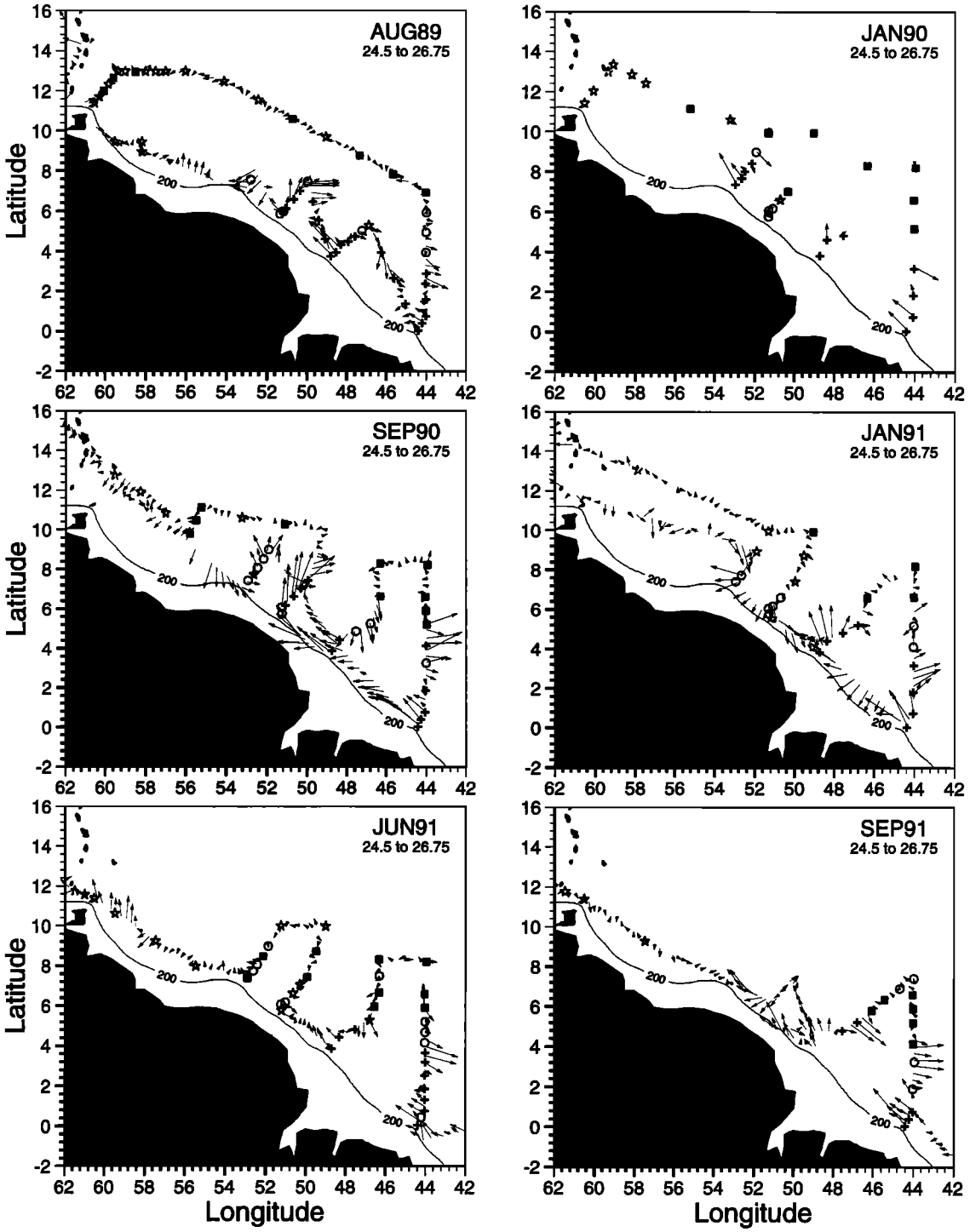

Figure 7. Same as Figure 6, but for the 24.5 to 26.75 density layer.

are representative of the NBUC, a boundary current found as far south as 10°S [*Stramma et al.*, 1995; *Schott et al.*, 1995]. The NBUC is spatially coincident with the increased vertical separation between the 24.5 and 26.75 isopycnal surfaces, characteristic of the reduced temperature gradients of the equatorial thermostad. The highest-velocity isotachs indicate that the NBUC is narrower than the NBC.

During all cruises, eastward flows associated with the NECC and NEUC are located to the north of the NBC/NBUC along 44°W (Figure 8). As described earlier, these zonal flows are composed, in part, of NBC/NBUC waters that have separated from the boundary in the retroflection. The NECC is typically characterized by a subsurface velocity core, centered around 60–80 m depth. This subsurface core is probably the signature of a current flowing against an opposing surface wind (i.e., the trades). Maximum velocities of about 100–120 cm s^{-1} are observed in the summer cruises, and significantly weaker ones (50–70 cm s^{-1}) are observed in the two January cruises.

As described by W94, during August 1989 the core of the upper layer NECC is markedly displaced (by at least 200 km)

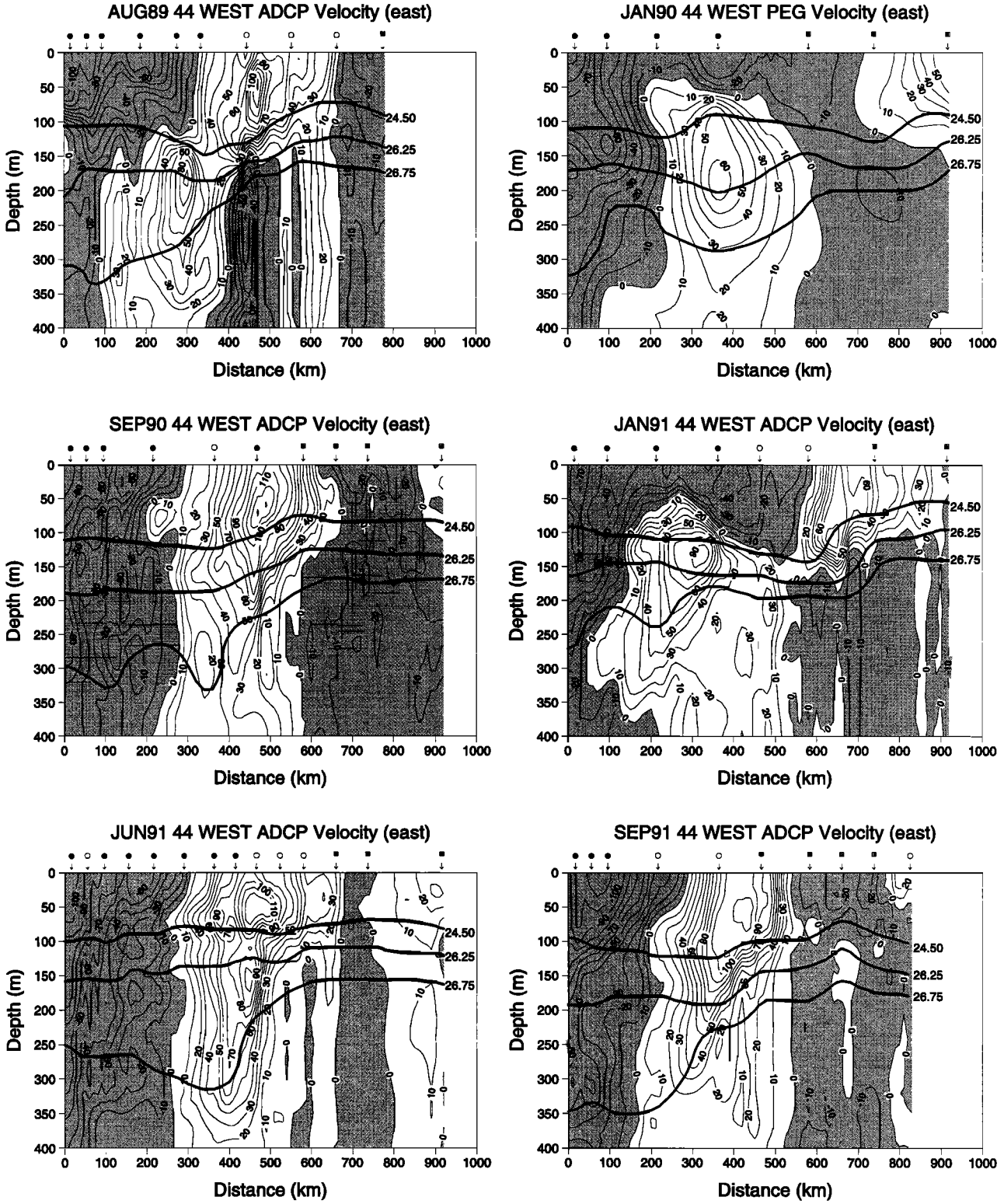

Figure 8. Vertical sections of eastward velocity component (in centimeters per second) along 44°W for the six cruises. Distance is in degrees latitude from the transect origin at 0°, 44°W. Selected isopycnal surfaces are superimposed. Station locations and water mass symbols are listed along the top axes.

from the core of the lower layer NEUC (Figure 8). The NECC and NEUC cores are also separated during the January 1990 and January 1991 transects. During the June 1991 cruise, although the NECC and NEUC are aligned, there is a separate core (>90 cm s^{-1}) of the NEUC on the 26.25 isopycnal. However, during September 1990 and September 1991 the two eastward currents are aligned in the vertical and there is no distinct NEUC core present in the lower layer. The deepening of the 26.75 isopycnal (indicative of the thermostad) and the deepening of the isotachs beneath the surface NECC to about

Table 2. Volume Transport Across 44°W

Cruise	NBC	NBUC	NECC	NEUC
August 1989	13.8	3.3	17.6	10.9
January 1990	11.0	11.5	3.5[a]	17.0
September 1990	11.5	13.3	18.9	18.1
January 1991	10.2	5.9	10.2[a]	12.9
June 1991	12.5	14.2	17.0	21.6
September 1991	14.3	11.4	20.6	11.5
Average	12.2 ± 1.6	9.9 ± 4.3	14.6 ± 6.5	15.3 ± 4.2

Transports are in sverdrups. Abbreviations are NBC, North Brazil Current; NBUC, North Brazil Undercurrent; NECC, North Equatorial Countercurrent; and NEUC, North Equatorial Undercurrent.
[a]Northern boundary of current was not crossed.

300 to 400 km along the transect indicate that the NEUC is nevertheless still present during these cruises. To the north of the NECC/NEUC countercurrents along 44°W, there is commonly westward flow associated with the southern edge of the NEC (Figure 8). The NEC is most clearly evident in the summer/fall cruises when the NECC is farthest south.

4.3. Current Transports at 44°W

Current transports have been computed based on the isopycnal layers, with the upper layer NBC and NECC defined as being located above the 24.5 isopycnal and the lower layer NBUC and NEUC defined as being between the 24.5 and 26.75 isopycnal surfaces. There is, of course, some overlap between the actual observed current fields and the isopycnal depths, but, for the most part, the current cores are located between these surfaces. For purposes of the transport computations the currents have been delineated in the horizontal, along-transect direction by where the perpendicular velocity component changes sign, i.e., where the integrated transport within each density layer reaches a maximum or minimum.

Transports for the NBC and NBUC are listed in Table 2. The mean transport of the NBC for the six cruises is 12.2 ± 1.6 Sv, and the mean NBUC transport is 9.9 ± 4.3 Sv, for a total combined mean northwestward cross-equatorial inflow of 22.1 ± 4.5 Sv for the two density layers. We note that in all cruises, westward flows of some 10–40 cm s^{-1} are still observed at the 26.75 σ_θ level. Thus the observed NBC/NBUC transports are likely to be somewhat underestimated.

As listed in Table 2, there does appear to be some seasonality to the transports of the NBC and the NBUC. For the four spring/summer cruises (i.e., August 1989, September 1990, June 1991, and September 1991) the mean NBC transport is 13.0 ± 1.3 Sv, as opposed to 10.6 ± 0.6 Sv for the two winter cruises (January 1990 and January 1991). Similarly, the spring/summer NBUC transport is 10.6 ± 5.0 Sv as opposed to 8.7 ± 4.0 Sv for the winter cruises. Averaging the four spring/summer total transports gives a somewhat larger flow (23.6 ± 4.4 Sv) than the average of the two January transports (19.1 ± 4.2 Sv).

Transports for the eastward counterflows, the NECC and NEUC, are also given in Table 2. The mean NECC transport across 44°W is 14.6 ± 6.5 Sv, and the mean NEUC transport is 15.3 ± 4.2 Sv. The four spring/summer NECC transports are very similar in magnitude, with a mean of 18.5 ± 1.6 Sv. The winter mean NECC transport is 6.9 ± 4.7 Sv, but this is also likely an underestimate, as the NECC was displaced northward during the January cruises and the section did not cross the entire eastward flow. Thus we cannot speak of seasonality of NECC transport from these data. The mean spring/summer NEUC transport is 15.5 ± 5.2 Sv, and the mean NEUC transport of the two winter cruises is 15.0 ± 2.9 Sv.

The combined eastward transports of the NECC and NEUC, with a mean of 30.0 ± 7.3 Sv, are almost always greater than the total alongshore NBC and NBUC boundary transport (22.1 ± 4.5 Sv), which is their primary source (Table 3). The mean transport "deficit" of the NECC/NEUC, i.e., that part of their transport that is not supplied by the NBC/NBUC, is therefore 7.9 Sv. The transport differences between the NBC/NBUC and the NECC/NEUC sums range from −1.6 Sv during January 1990 to 12.2 Sv during September 1990.

One cause for this transport deficit may be missed NBC/NBUC transport along the shelf, shoreward of the 200-m isobath. However, estimates of this flow [*Johns et al.*, 1998] are only 2 to 3 Sv. Thus, with either partial or total retroflection of the NBC/NBUC, the larger observed differences from the present study suggest the addition of northern origin waters retroflecting cyclonically from the NEC to achieve the total transport of the NECC and NEUC zonal flows. This was also noted by W94 for the August 1989 cruise. The presence of ETW along the northern edges of the 44°W section supports this conclusion.

4.4. NBC Rings

Fratantoni et al. [1995] describe the temporal evolution of a NBC ring. This evolution is characterized by an intrusion of the NBC retroflection northwestward along the coastline, with a large meander subsequently developing on the offshore side of the retroflection. Eventually, the ring separates and drifts northwestward toward the Caribbean Sea. Although we have no continuous record of such a ring, the six cruises available nevertheless provide some observational insight into the evolution of such features.

W94 describe a recently separated eddy observed during August 1989. This eddy is characterized in both layers by southwestward flow just poleward of the northernmost CTD section on Figures 6 and 7. Water mass properties and current vectors also suggest an eddy has recently separated during the January 1990 cruise. At these apparent early stages of separation, the velocity fields shown in Figures 6 and 7 suggest little eddy spin-down.

Richardson et al. [1994] describe the trajectory of a satellite-tracked surface drifter that was deployed into the central region of the retroflection. The exact separation time of the associated ring can only be specified to sometime during November to December 1990. Assuming that the drifter remained within the ring, as suggested by its looping motion, the ring was

Table 3. Volume Transport Across 44°W for Combined NBC/NBUC and NECC/NEUC

Cruise	NBC + NBUC	NECC + NEUC	Δ
August 1989	17.1	28.5	11.4
January 1990	22.1	20.5	−1.6
September 1990	24.8	37.0	12.2
January 1991	16.1	23.1	7.0
June 1991	26.7	38.6	11.9
September 1991	25.7	32.1	6.4
Average	22.1 ± 4.5	30.0 ± 7.3	7.9 ± 5.3

Transports are in sverdrups. Here Δ denotes the difference between the inflow to the study area (NBC + NBUC) and the outflow (NECC + NEUC).

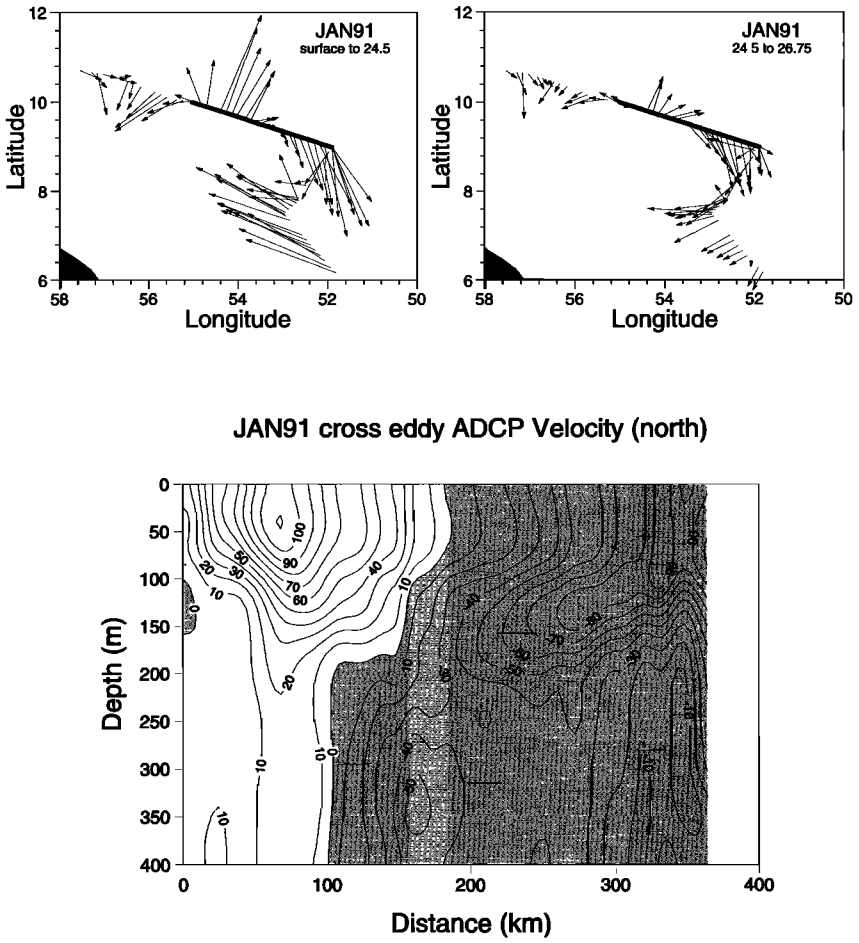

Figure 9. January 1991 horizontal maps of ADCP velocity for the (top) upper and lower density layers and (bottom) northward velocity section from the solid line transect at top, passing through a recently separated North Brazil Current (NBC) eddy. Isopycnal layers were computed from the CTDO2 stations nearest to the transect.

located at approximately 9°N, 54°W during January 1991, close to the cruise track line occupied during that month (Figure 2). The vertical section of velocity obtained from the transect closest to the buoy trajectory is shown in Figure 9. The velocity field is very similar to the structure within the NBC retroflection at 44°W (Figure 8). Maximum speeds in the eddy are similar to the speeds observed in the NBC retroflection with a maximum of about 100 cm s^{-1}. Thus a separated eddy can retain its velocity properties some months after separation. Unfortunately, no $CTDO_2$ data are available along this ADCP transect through the NBC eddy.

5. Discussion

On the basis of the transports estimated from the shipboard ADCP and Pegasus sections and the associated temperature, salinity, and dissolved oxygen properties, we have constructed transport schematics representing idealized pathways of current flows in the study region. These schematic transport diagrams were constructed for the two density layers to examine further the transport and water mass sources of the NBC, NBUC, NECC, and NEUC.

Although several closed regions are delineated by the cruise tracks of the various cruises, there are a number of reasons why one would not expect to find an exact mass balance in this region even in such closed volumes. First, the measurements are not truly synoptic. A typical cruise required about 3 weeks to complete, and large temporal variability has been observed in the current structure in this region. For example, the NBC exhibits large oscillations with 40- to 70-day periods [*Johns et al.*, 1990; *Schott et al.*, 1993; *Colin et al.*, 1994]. Such variability could account for as much as 15% of the transport measured over the duration of the surveys. Higher-frequency vertical motions (e.g., inertial, tidal) of isopycnals can also affect transport integrals. Second, the assumption has been made that no vertical transport occurs between the density layers. Modeling results suggest that such motions may be present in the region [*Philander and Pacanowski*, 1986; *Schott and Boning*, 1991], and observations show it to be an area of coastal upwelling and relatively important vertical mixing [*Schmitt et al.*, 1987; *Moum et al.*, 1989; *Gouriou and Reverdin*, 1992]. Third, no measurements from these cruises are available over the coastal shelf, with the closest measurements only reaching the 200-m isobath. Strong currents over the shelf have been observed north of the equator and west of 44°W. Various estimates of this coastal transport are all in the 1- to 4-Sv range [*Candela et al.*, 1992; *Friedrichs*, 1992; *Johns et al.*, 1998].

The schematics (Figures 10 and 11) were constructed to agree as closely as possible to the observed transports along the

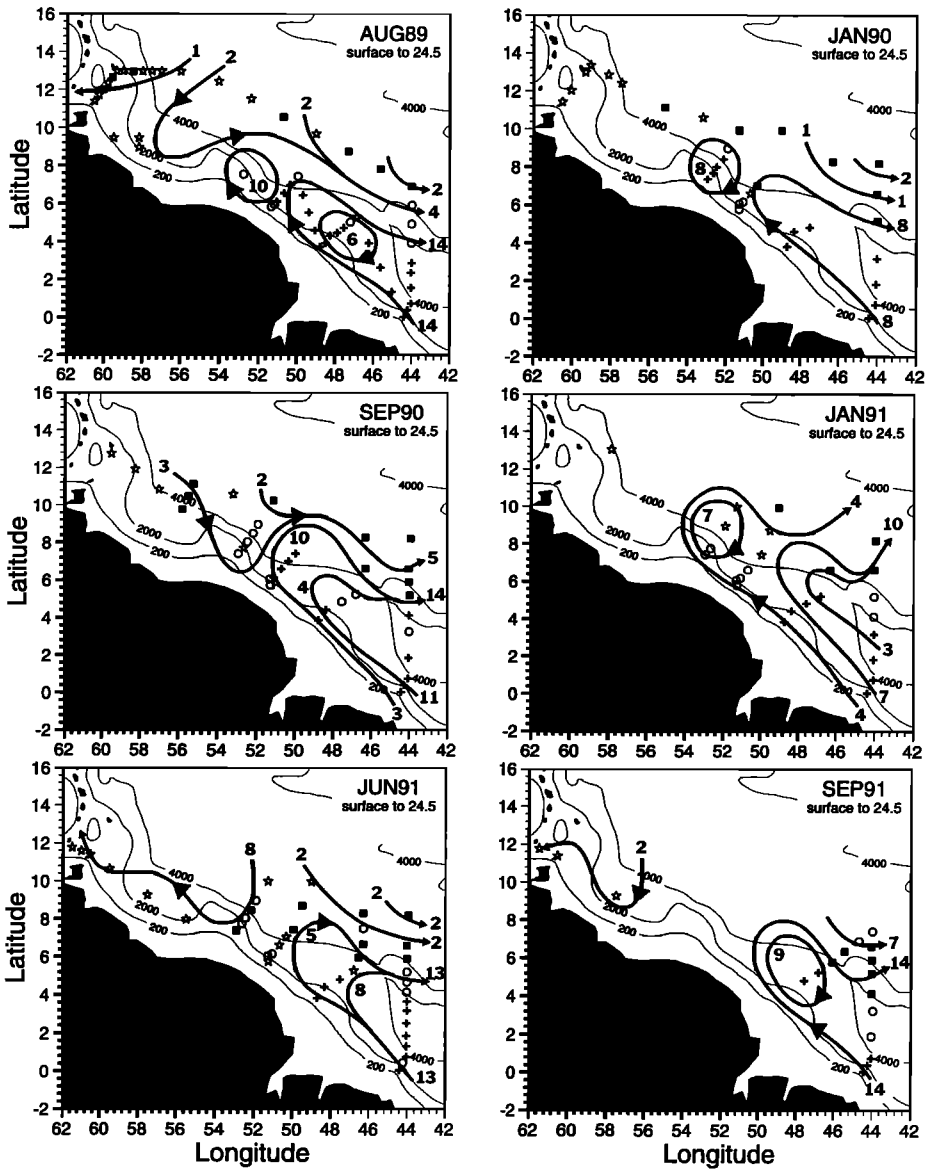

Figure 10. Schematics of estimated volume transport in sverdrups (1 Sv = 10^6 m^3 s^{-1}) for the upper layer, between the surface and the 24.5 isopycnal, for the six cruises. Water mass symbols as defined in Figure 4 are also given.

44°W section; they represent subjectively drawn averages of the observations elsewhere due to the synopticity concerns described earlier. The schematics were also constructed to have all the boundary transport retroflect into the NECC and NEUC (Figures 10 and 11). This total retroflection is based on the absence of any southern origin water north of the retroflection, except within the closed eddies observed during August 1989, January 1990, and January 1991 (Figures 6 and 7). The January 1991 case is ambiguous, in that it is difficult to discern from the currents the exact stage of eddy separation (Figures 6 and 7). On the basis of water mass properties, we assume nearly complete separation of both levels (Figures 10 and 11). As mentioned earlier, the absence of stations shoreward of the 200-m isobath precludes the identification of any continuous coastal flows that may advect southern origin water masses. Nevertheless, the estimates of such coastal transport are an order of magnitude less than the observed NECC/NEUC combined transports from the present study.

In summary, on the basis of the transport schematics, the dominant feature is the NBC/NBUC retroflection. The NECC and NEUC are also found in all six cruises (Figures 10 and 11). During all cruises these zonal countercurrents are fed by the anticyclonic retroflection of the NBC/NBUC (southern hemisphere origin) and by a cyclonic retroflecting branch of the NEC (northern hemisphere origin). Mixed water mass characteristics develop among the boundaries between the source water masses. Except for January 1990, the NECC is composed of waters from both hemispheres. However, the shear characteristics of the upper layer flow during this month suggest that the near-surface currents are associated with the NEUC rather than the NECC.

During all the other months the relative amount of southern origin waters retroflected offshore in the upper layer remains relatively constant at about 14 Sv. The relative proportion of mixed to pure southern waters is also similar, without about 10 Sv of unmixed and 5 Sv of mixed transport typically found in

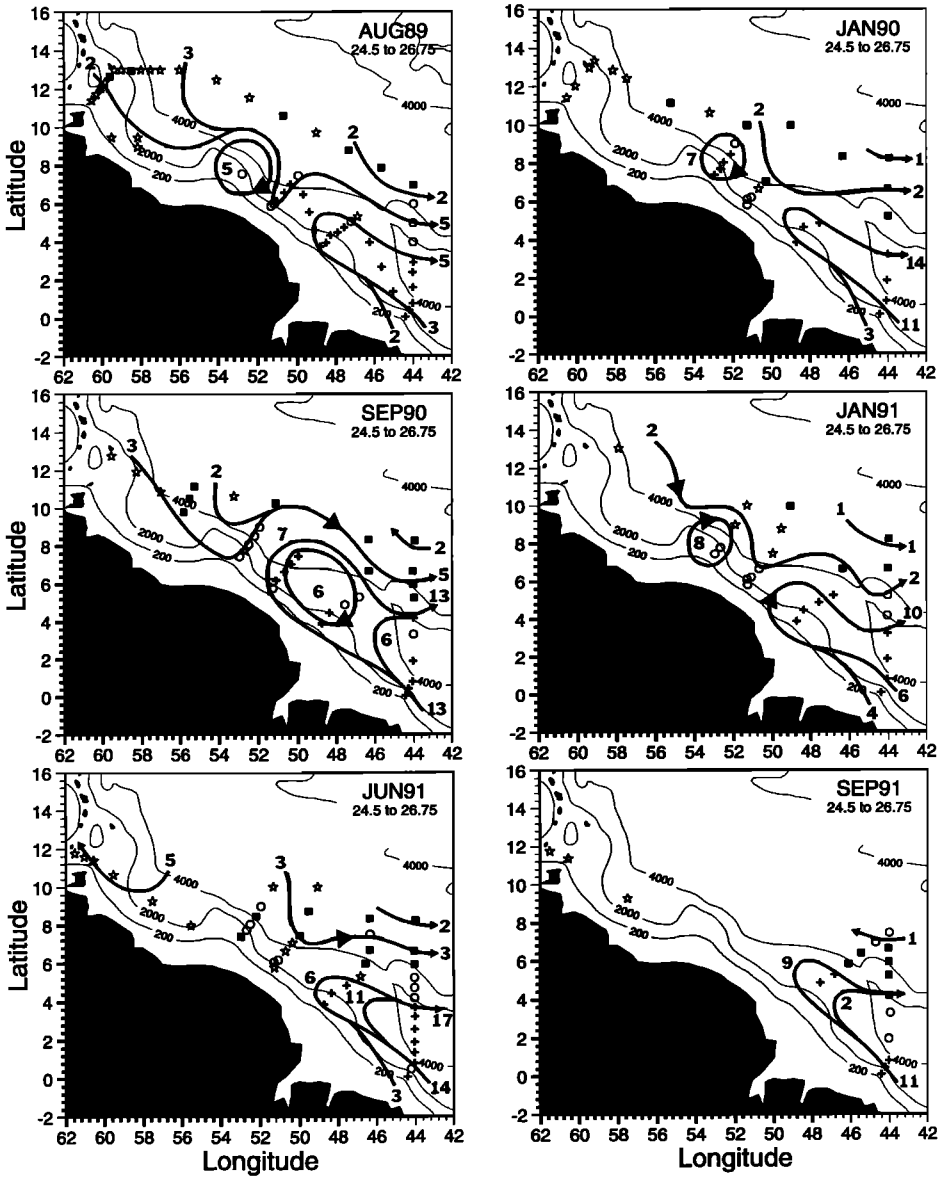

Figure 11. Same as Figure 10, except for the lower layer between the isopycnal surfaces 24.5 and 26.75.

the NECC. Similarly, during the summer cruises, the total amount of northern origin water transported in the NECC is relatively constant at about 5 to 7 Sv. As indicated before, the NECC transport for the January cruises is an underestimate, as the flow extended beyond the northern end of the sections. Thus the only general statement that can be made about NECC transport is that during the summer it is fed by approximately two thirds southern and one third northern waters.

The situation is different in the lower density layer. Except for August 1989, the total NEUC transport that includes southern hemisphere water is remarkably constant (i.e., 10 to 14 Sv southern and 1 to 3 Sv mixed). The northern origin contribution, again except for August 1989, is also relatively stable at about 1 to 3 Sv of northern transport. Thus, throughout these six cruises, the NEUC is primarily supplied by transport from the retroflecting NBUC, with a smaller contribution to the flow provided by the retroflecting NEC.

We indicate that the retroflected transport in the lower layer is entrained into the NEUC rather than the EUC. This assumption is based on the velocity and density structure along 44°W, which shows a subsurface velocity maximum within the NEUC at depths greater than 100 m for all but the two September cruises (which, because of the alignment of the NECC and NEUC, have no subsurface velocity core). The core of the EUC in the Atlantic typically occurs at about 100 m. The subsurface eastward current also is observed on the northern side of the equatorial thermostad (Figure 8). The NEUC exhibits similar characteristics farther to the east [*Cochrane et al.*, 1979]. However, we cannot discount splitting of this velocity core to the east with some of the flow joining the EUC. Such a separation is necessary to complete the shallow overturning cell hypothesized by *Gu and Philander* [1997] for the Pacific Ocean as described previously.

6. Summary

In summary, the results presented above provide both new perspectives on and additional quantification of earlier results.

Of course, it must be kept in mind that there were only six cruises, with none in the early spring or late fall owing to the lack of available ship time. There was also incomplete data coverage of the coastal currents over the shelf and incomplete coverage north of the NBC retroflection. Nevertheless, certain points remain clear.

1. The average transport of the NBC/NBUC system is 22.1 ± 4.5 Sv. *Schott et al.* [1993] estimated a mean NBC/NBUC transport for the upper 300 m of 23.8 Sv from current meter moorings deployed at the same time as the ADCP cruises. The ADCP data provide better spatial but poorer temporal resolution than the mooring data. The similar estimates thus suggest a convergence on the mean transport.

2. The average NBC/NBUC transport for the four summer cruises is 23.6 Sv, and for the two winter cruises it is 19.1 Sv. These ADCP-derived estimates are consistent with the annual cycle derived by *Schott et al.* [1993]; however, their significance is limited by the large higher-frequency variability observed in the current meter records.

3. A retroflection in both layers occurs during all six cruises. These velocity data are thus consistent with the climatological temperature data given by *Molinari and Johns* [1994]. The mean monthly temperature distributions in the latter study all show a retroflection. Both data sets thus bring into question the existence of a continuous NBC away from the shelf from the equator to the Caribbean.

4. Consistent with the previous findings, the NECC and NEUC are observed at 44°W during the six cruises. The combined mean transport of these eastward flows is 30.0 ± 7.3 Sv.

5. The difference in transport between the NBC/NBUC and NECC/NEUC systems is provided by a portion of the NEC that retroflects at the boundary. This combining of southern hemisphere and northern hemisphere water masses provides a mechanism for forming water masses with different characteristics and is indicative of the role of the study region as a "blender" of northern and southern origin waters.

Acknowledgments. We gratefully acknowledge P. Richardson, W. Johns, D. Fratantoni, F. Schott, C. Colin, and F. Bub for helpful discussions and communications of unpublished results. Special thanks to the officers and crew of NOAA's *Malcolm Baldrige* and *Mt. Mitchell*. A portion of this work was conducted during a 1-year visit by B. Bourles to NOAA's Atlantic Oceanographic and Meteorological Laboratory in Miami, Florida.

References

Brown, W. S., W. E. Johns, K. D. Leaman, J. P. McCreary, R. L. Molinari, P. L. Richardson, and C. Rooth, A Western Tropical Atlantic Experiment (WESTRAX), *Oceanography*, *5*(1), 73–77, 1992.

Bruce, J. G., J. L. Kerling, and W. H. Beatty III, On the north Brazilian eddy field, *Prog. Oceanogr.*, *14*, 57–63, 1985.

Candela, J., R. C. Beardsley, and R. Limeburner, Separation of tidal and subtidal currents in ship-mounted acoustic Doppler current profiler observations, *J. Geophys. Res.*, *97*, 769–788, 1992.

Cochrane, J. D., F. J. Kelly Jr., and C. R. Olling, Subthermocline countercurrents in the western equatorial Atlantic Ocean, *J. Phys. Oceanogr.*, *9*, 724–738, 1979.

Colin, C., and B. Bourles, Western boundary currents and transports off French Guiana as inferred from Pegasus observations, *Oceanol. Acta*, *17*(2), 143–157, 1994.

Colin, C. B., B. Bourles, R. Chuchla, and F. Dangu, Western boundary current variability off French Guiana as observed from moored current measurements, *Oceanol. Acta*, *17*(4), 345–354, 1994.

Csanady, G. T., A zero potential vorticity model of the North Brazilian Current, *J. Mar. Res.*, *43*, 553–579, 1985.

Didden, N., and F. A. Schott, Eddies in the North Brazil Current retroflection region observed by Geosat altimetry, *J. Geophys. Res.*, *98*, 20,121–20,131, 1993.

Emery, W. J., and J. S. Dewar, Mean temperature-salinity, salinity-depth and temperature-depth curves for the North Atlantic and the North Pacific, *Prog. Oceanogr.*, *11*, 219–305, 1982.

Flagg, C. N., R. L. Gordon, and S. McDowell, Hydrographic and current observations on the continental slope and shelf of the western equatorial Atlantic, *J. Phys. Oceanogr.*, *16*, 1412–1429, 1986.

Fratantoni, D. M., W. E. Johns, and T. L. Townsend, Rings of the North Brazil Current: Their structure and behavior inferred from observations and a numerical simulation, *J. Geophys. Res.*, *100*, 10,633–10,654, 1995.

Friedrichs, M. A. M., Meridional circulation in the tropical North Atlantic, M. S. thesis, Mass. Inst. of Technol. and Woods Hole Oceanogr. Inst. Joint Program in Oceanogr., Woods Hole, Mass., 1992.

Garzoli, S. L., The Atlantic North Equatorial Countercurrent: Models and observations, *J. Geophys. Res.*, *97*, 17,931–17,946, 1992.

Gordon, A. L., Interocean exchange of thermocline water, *J. Geophys. Res.*, *91*, 5037–5046, 1986.

Gouriou, Y., and G. Reverdin, Isopycnal and diapycnal circulation of the upper equatorial Atlantic Ocean in 1983–1984, *J. Geophys. Res.*, *97*, 3543–3572, 1992.

Gu, D., and S. G. H. Philander, Interdecadal climate fluctuations that depend on exchanges between the tropics and extratropics, *Science*, *275*, 805–807, 1997.

Johns, E., and A. M. Wilburn, Hydrographic observations in the western tropical and subtropical North Atlantic Ocean: Atlantic Climate Change Program (ACCP) and Western Tropical Atlantic Experiment (WESTRAX) during 1990, *NOAA Data Rep., ERL AOML-22*, 102 pp., Natl. Oceanic and Atmos. Admin., Silver Spring, Md., 1993a.

Johns, E., and A. M. Wilburn, Hydrographic observations in the western tropical and subtropical North Atlantic Ocean: Atlantic Climate Change Program (ACCP) and Western Tropical Atlantic Experiment (WESTRAX) during 1991, *NOAA Data Rep. ERL AOML-23*, 82 pp., Natl. Oceanic and Atmos. Admin., Silver Spring, Md., 1993b.

Johns, W. E., T. N. Lee, F. A. Schott, R. J. Zantopp, and R. H. Evans, The North Brazil Current retroflection: Seasonal structure and eddy variability, *J. Geophys. Res.*, *95*, 22,103–22,120, 1990.

Johns, W. E., T. N. Lee, R. C. Beardsley, J. Candela, R. Limeburner, and B. Castro, Annual cycle and variability of the North Brazil Current, *J. Phys. Oceanogr.*, *28*, 103–128, 1998.

Joyce, T. M., On in-situ "calibration" of shipboard ADCPs, *J. Atmos. Oceanic Technol.*, *6*, 169–172, 1989.

Leaman, K. D., and P. S. Vertes, The Subtropical Atlantic Climate Study (STACS), 1982: Summary of RSMAS Pegasus observations in the Florida Straits, *RSMAS Tech. Rep. 83012*, Rosenstiel School of Mar. and Atmos. Sci., Univ. of Miami, Miami, Fla., 1983.

Leaman, K. D., R. L. Molinari, and P. S. Vertes, Structure and variability of the Florida Current at 27–28°N: April 1982–July 1984, *J. Phys. Oceanogr.*, *17*, 565–583, 1987.

Leaman, K. D., P. S. Vertes, L. P. Atkinson, T. N. Lee, P. Hamilton, and E. Waddel, Transports, potential vorticity and current/temperature structure across Northwest Providence and Santaren Channels and the Florida Current off Cay Sal Bank, *J. Geophys. Res.*, *100*, 8561–8569, 1995.

Metcalf, W., Shallow currents along the northeastern coast of South America, *J. Mar. Res.*, *26*, 232–243, 1968.

Metcalf, W., and M. C. Stalcup, Origin of the Atlantic Equatorial Undercurrent, *J. Geophys. Res.*, *72*, 4959–4975, 1967.

Molinari, R. L., and E. Johns, Upper layer temperature structure of the western tropical Atlantic, *J. Geophys. Res.*, *99*, 18,225–18,233, 1994.

Moum, J. N., D. R. Caldwell, and C. A. Paulson, Mixing in the equatorial surface layer and thermocline, *J. Geophys. Res.*, *94*, 2005–2021, 1989.

Philander, S. G. H., and R. C. Pacanowski, A model of the seasonal cycle in the tropical Atlantic Ocean, *J. Geophys. Res.*, *91*, 14,192–14,206, 1986.

Pollard, R., and J. Read, A method for calibrating ship-mounted acoustic Doppler current profiles, and the limitations of gyrocompasses, *J. Atmos. Oceanic Technol.*, *6*, 859–865, 1989.

Richardson, P. L., and G. Reverdin, Seasonal cycle of velocity in the

Atlantic NECC as measured by surface drifters, current meters and ship drifts, *J. Geophys. Res.*, *92*, 3691–3708, 1987.

Richardson, P. L., and D. Walsh, Mapping climatological seasonal variations of surface currents in the tropical Atlantic using ship drifts, *J. Geophys. Res.*, *91*, 10,537–10,550, 1986.

Richardson, P. L., G. Hufford, R. Limeburner, and W. Brown, North Brazil Current retroflection eddies, *J. Geophys. Res.*, *99*, 5081–5093, 1994.

Routt, J. A., and W. D. Wilson, Shipboard acoustic Doppler current profiler data collected during the Western Tropical Atlantic Experiment (WESTRAX), 1991, *NOAA Tech. Memo., ERL AOML-72*, Natl. Oceanic and Atmos. Admin., Silver Spring, Md., 1992.

Schmitt, R. W., H. Perkins, J. D. Boyd, and M. C. Stalcup, C-Salt: An investigation of the thermohaline staircase in the western tropical North Atlantic, *Deep Sea Res., Part A*, *34*(10), 1655–1665, 1987.

Schmitz, W. J., and M. S. McCartney, On the North Atlantic circulation, *Rev. Geophys.*, *31*(1), 29–49, 1993.

Schmitz, W. J., and P. L. Richardson, On the source of the Florida Current, *Deep Sea Res., Part A*, *38*, suppl. 1, S379–S409, 1991.

Schmitz, W. J., J. R. Luyten, and R. W. Schmitt, On the Florida Current T/S envelope, *Bull. Mar. Sci.*, *53*(3), 1048–1065, 1993.

Schott, F. A., and C. W. Boning, The WOCE model in the western equatorial Atlantic: Upper layer circulation, *J. Geophys. Res.*, *96*, 6993–7004, 1991.

Schott, F. A., J. Fischer, J. Reppin, and U. Send, On mean and seasonal currents and transports at the western boundary of the Equatorial Atlantic, *J. Geophys. Res.*, *98*, 14,353–14,368, 1993.

Schott, F. A., L. Stramma, and J. Fischer, The warm water inflow into the western tropical Atlantic boundary regime, spring 1994, *J. Geophys. Res.*, *100*, 24,745–24,760, 1995.

Send, U., Accuracy of current profile measurements: Effects of tropical and midlatitude internal waves, *J. Geophys. Res.*, *99*, 16,229–16,236, 1994.

Silveira, I. C. A., L. B. de Miranda, and W. S. Brown, On the origins of the North Brazil Current, *J. Geophys. Res.*, *99*, 22,501–22,512, 1994.

Spain, P. F., D. L. Dorson, and H. T. Rossby, Pegasus: A simple acoustically-tracked velocity profiler, *Deep Sea Res., Part A*, *28A*, 1553–1567, 1981.

Stramma, L., J. Fischer, and J. Reppin, The North Brazil Undercurrent, *Deep Sea Res., Part I*, *42*, 773–795, 1995.

Wilburn, A. M., E. Johns, and M. H. Bushnell, Current velocity and hydrographic observations in the Subtropical North Atlantic Ocean: Subtropical Atlantic Climate Studies (STACS), 1989, *NOAA Data Rep., ERL AOML-18*, 97 pp., Natl. Oceanic and Atmos. Admin., Silver Spring, Md., 1990.

Wilson, W. D., and J. A. Routt, Shipboard acoustic Doppler current profiler data collected during the Subtropical Atlantic Climate studies (STACS) project (1989–1990), *NOAA Tech. Memo., ERL AOML-71*, Natl. Oceanic and Atmos. Admin., Silver Spring, Md., 1992.

Wilson, W. D., E. Johns, and R. L. Molinari, Upper layer circulation in the western tropical North Atlantic Ocean during August 1989, *J. Geophys. Res.*, *99*, 22,513–22,523, 1994.

Worthington, L. V., On the North Atlantic circulation, *Johns Hopkins Oceanogr. Stud.*, *6*, 110 pp., 1976.

B. Bourles, Centre ORSTOM de Brest, B.P. 70, 29280 Plouzane, France.

E. Johns, R. L. Molinari, and W. D. Wilson, NOAA/AOML/PHOD, 4301 Rickenbacker Causeway, Miami, FL 33149. (Johns@aoml.noaa.gov); (wilson@aoml.noaa.gov)

K. D. Leaman, RSMAS/UM, 4600 Rickenbacker Causeway, Miami, FL 33149.

(Received November 26, 1997; revised July 2, 1998;
accepted August 9, 1998.)